TENTH AUSTRALASIAN FLUID MECHANICS
CONFERENCE - UNIVERSITY OF MELBOURNE
11-15 DECEMBER 1989

FINITE ELEMENT SIMULATION OF THE KINEMATICS OF THE ASPIRATED JET

D.J. HASBERG and Y.L. YEOW

Department of Chemical Engineering
University of Melbourne, Parkville, Vic. 3052
AUSTRALIA

INTRODUCTION

A great deal of interest has been generated in the last few years regarding the extensional flow of dilute polymeric liquids and their flow properties. Examples of industrially important applications include the manufacture of synthetic fibres by fibre spinning, enhanced oil recovery by polymer flooding, and the flow of modified lubricants in bearings.

One of the tools that has been used by investigators to obtain measurements of the elongational properties of such polymer solutions is the Aspirated Jet Technique, shown schematically in figure 1(a). The principle of operation of the aspirated jet viscometer is relatively simple. Fluid flows from a constant head reservoir through a capillary (the outlet capillary) and is aspirated into a smaller diameter suction capillary by the inception of a vacuum.

The volumetric flow through the outlet capillary is dependant on the pressure in the upper reservoir and the normal stress at the exit of the outlet capillary. Through the application of the aspirated suction capillary, the flow through the outlet capillary is significantly increased due to the increased normal stress in the fluid jet. From a measurement of the volumetric flowrate through the outlet [1], with and without aspiration, it is possible to obtain a calculation of the average extensional stress, σ, at the outlet tube. The variation of the jet diameter with axial distance, z, can be recorded by photographic methods, and the average elongational rate, $\dot{\varepsilon}$, at any horizontal cross section of the fluid jet, can be obtained by numerical differentiation of the jet diameter with respect to the axial distance [2].

The apparent elongational viscosity is then given by:

$$\eta_{app} = \sigma/\dot{\varepsilon} \qquad (1)$$

The key underlying assumption in this analysis is that the flow is fully-developed in the Eulerian sense, i.e. the axial velocity at any horizontal section is uniform and not a function of radial position, r. This simplifying assumption is valid for the gravity-drawn, or unaspirated jet, but for aspirated jets, where jets as short as two to three outlet capillary diameters (D_o) have been used, the uniform velocity profile becomes unteneable.

The validity of this assumption has not been systematically checked. An attempt [3] has been made to obtain local velocity and deformation rates using a flow visualisation technique, clearly showing non-uniform velocity profiles in the jet.

It is the aim of this work to obtain a detailed mapping of the velocity field in the fluid jet using a finite element technique, under conditions closely approximating those encountered in experimental measurements.

METHOD

Figure 1(b) illustrate the general arrangement of the finite element mesh of the aspirated jet used for the numerical simulation. The normal and tangential stress on the jet surface were set equal to zero, as the surface tension can be assumed to be negligible for this type of problem [2]. A fully developed parabolic velocity profile was imposed on both the inlet an outlet of the finite element mesh.

The finite element computation for the aspirated jet is complicated by the presence of the fluid/air interface. The position of this surface is not known and has to be determined as an integral part of the computational exercise. This class of problem is usually referred to as a 'free boundary' problem. In this work, an iterative scheme was used to locate the fluid/air interface.

For axisymmetric flow, where $u_\theta = 0$, u_r and u_z can be expressed in terms of the stream function, Ψ [4],

$$u_r = 1/r \; \delta\Psi/\delta z \qquad (2)$$

$$u_z = -1/r \; \delta\Psi/\delta r \qquad (3)$$

The fluid/air interface is a stream line. For convenience, Ψ is taken to be identically zero on this interface. An initial guess of this interface is made. Finite element methods are then used to solve the governing equations, i.e. the continuity equation and the Cauchy equation of motion. Unless the initial guess of these interface location coincides with the true interface, Ψ will not be zero. If at any point on the interface, the stream function deviates from zero by an amount $\Delta\Psi$, then according to (3), the adjustment in radial position, Δr, needed to drive Ψ towards zero is given by:

$$\Delta r = \Delta\Psi/-u_z \, r \qquad (4)$$

The new radial coordinate of the free surface is given by

$$r_{new} = r_{old} - f\,\Delta r \qquad (5)$$

where f is a relaxation factor, typically ≈ 0.1. A small value for f is often used to ensure convergence of the solution. This procedure was repeated until $[\Delta\Psi]$ was less than 10^{-6}. Typically, in the order of 10 to 15 iterations were required before convergence.

RESULTS

Three different geometries of aspirated jet were investigated:

(i) A long jet, 4:1 contraction ($D_o/D_s = 4$), of length $10D_s$.

(ii) Two shorter jets, 2:1 and 4:1 contraction, of length $2.5D_s$.

The fluid was assumed to have either a constant viscosity (Newtonian) or behave as a power law fluid, where stress, σ, and rate of strain, $\dot{\gamma}$, are related by an equation of the form,

$$\sigma = K\,(\dot{\gamma})^n \qquad (6)$$

where K and n are fluid parameters. In general, n>1 represents elongational thickening, and n<1 represents elongational thinning behaviour.

In figure 2, the magnitude of the velocity on the surface and central line are plotted against axial location, for a range of power law exponents for case (i). As can be seen, for n=1, the assumption of uniform velocity profile at any axial position, is reasonably valid for the main body of the jet; for between 60 - 70% of the jet length. As the fluid departs from Newtonian behaviour, i.e. n departs from unity, the validity of the assumption reduced to less than 50% of the jet length.

From the result for case (ii), as shown in figure 3, it can be seen that the absolute surface and centre velocities differ from one another for over 90% of the fibre length for the 2:1 contraction, and they are not equal at all for the 4:1 contraction.

As expected, this trend is also evident in the plots of elongation rate vs axial location for case (i)(figure 4) and case (ii)(figures 5,6). It is interesting to note in these plots that where the elongational rate at the surface near the outlet tube is greater than at the central line, this situation is reversed in the vicinity of the suction tube. Also, a maximum in the elongational rate is exhibited in the region close to the suction tube inlet, and to a lesser extent, a minimum can be detected at the outlet tube, for the centre line. These turning points can be attributed to die swell.

The effect of slip on the wall of the suction tube (tangential velocity non zero) has also been investigated, to simulate the entrainment of air into the suction tube, which has been observed in some experimental work. However, these results did not display the gross departure from uniform velocity profiles observed through flow visualisation [3], and did not vary significantly from the 'no wall-slip' aspirated jet simulations.

CONCLUSION

As a result of this numerical investigation into the velocity field contained in the aspirated jet, the assumption of uniform axial velocity profile, was found to have limited validity for the geometries investigated. The validity of the aspirated jet assumption improves with increasing jet length and decreasing contraction ratio. The limitations become more severe for non-Newtonian fluids, for which the technique was designed for.

ACKNOWLEDGEMENTS

D J Hasberg was supported by a Commonwealth Postgraduate Research Award while carrying out this investigation. The computations were carried out using 'POLYFLOW', a copy of which has been made available to the Department of Chemical Engineering, University of Melbourne, by Professor M J Crochet, Universite Catholique de Louvain, Lovain-a-Neuve, Belgium.

REFERENCES

1. Gupta, R.K., Sridhar, T., Proc. IX Intl. Cong. Rheology, p.71, 1984.

2. Ferguson, J., Hudson, N.E., J. Phys. E., 8, p.526, 1975.

3. Matthys, E.F., Khatami, M., Proc. X Intl. Cong. Rheology, 2, p.112, 1988.

4. Bird, R.B., Stewart, W.E., Lightfoot, E.N., Transport Phenomena, John Wiley & Sons, New York, 1960.

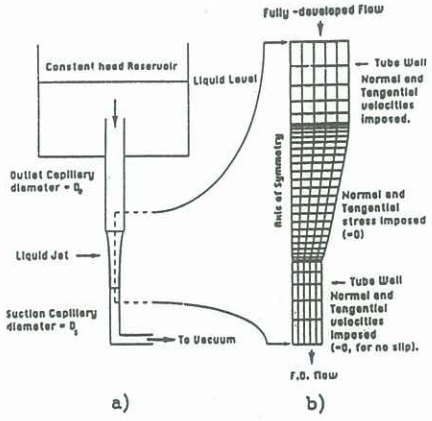

Figure 1 : a) Schematic diagram of the Aspirated Jet
b) Typical Finite Element mesh.

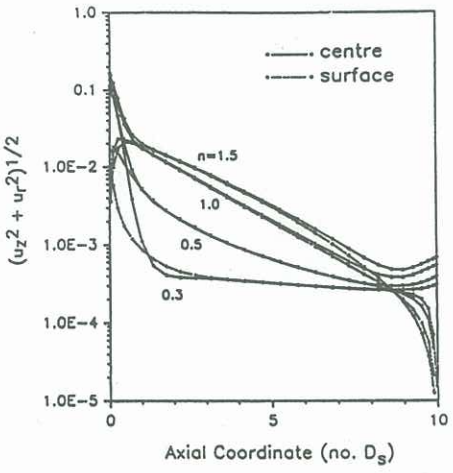

Figure 2. Plot of absolute velocity vs axial coordinate for case (i). Note that an axial coordinate of zero corresponds to the inlet of the suction tube.

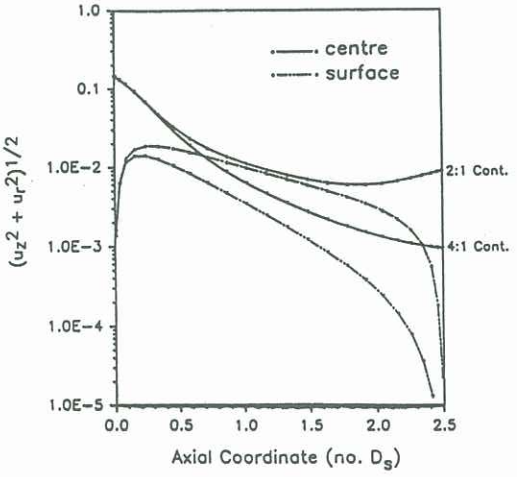

Figure 3. Plot of absolute velocity vs axial coordinate for case (ii).

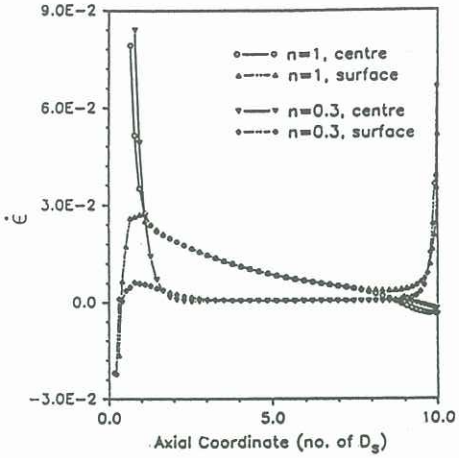

Figure 4. Plot of elongation rate vs axial coordinate for case (i).

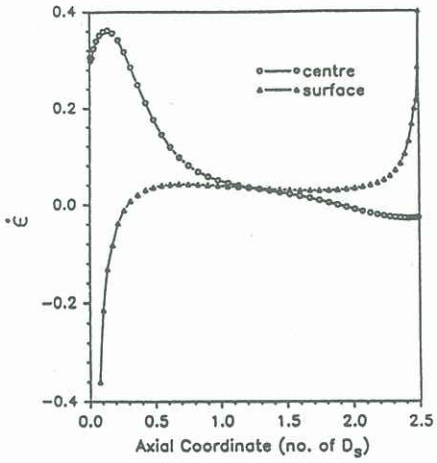

Figure 5. Plot of elongation rate vs axial coordinate for case (ii), 2:1 contraction.

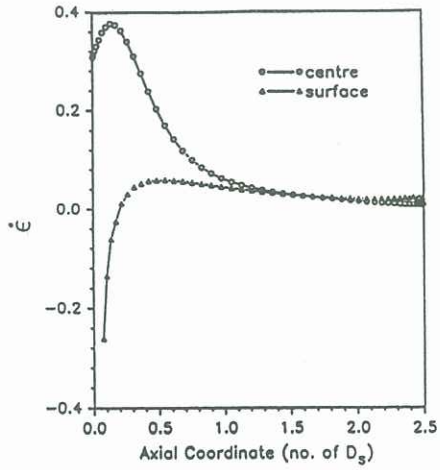

Figure 6. Plot of elongation rate vs axial coordinate for case (ii), 4:1 contraction.